

# Effects of Amino Substitution on the Excited State Hydrogen Transfer in Phenol: A TDDFT Study

Sang-su Kim, Minho Kim,<sup>†</sup> and Hyuk Kang\*

Department of Chemistry, Ajou University, Suwon 443-749, Korea. \*E-mail: hkang@ajou.ac.kr

<sup>†</sup>Division of Energy Systems Research, Ajou University, Suwon 443-749, Korea

Received March 22, 2009, Accepted May 9, 2009

When isolated phenol or a small phenol-solvent cluster is excited to the  $S_1$  state of  $\pi\pi^*$  character, the hydrogen atom of the hydroxyl group dissociates via a  $\pi\sigma^*$  state that is repulsive along the O-H bond. We computationally investigated the substitution effects of an amino group on the excited state hydrogen transfer reaction of phenol. The time-dependent density functional theory (TDDFT) with B3LYP functional was employed to calculate the potential energy profiles of the  $\pi\pi^*$  and the  $\pi\sigma^*$  excited states along the O-H coordinate, together with the orbital shape at each point, as the position of the substituent was varied. It was found that the amino substitution has an effect of lowering the  $\pi\sigma^*$  state and enhancing the excited state hydrogen transfer reaction.

**Key Words:** Excited state hydrogen transfer, Phenol, Aminophenol, Substitution effect, TDDFT

## Introduction

Phenol is a prototype of enols and heterocycles that undergo an excited state hydrogen transfer (ESHT), or concerted electron and proton transfer reaction.<sup>1,2</sup> When isolated phenol or a small phenol-solvent cluster is excited to the  $S_1$  state of  $\pi\pi^*$  character, the hydrogen atom of the hydroxyl group is dissociated or transferred to the solvent. The ESHT reaction is contrary to the traditional view that this cluster system will undergo an excited state proton transfer (ESPT) reaction as the  $pK_a$  of this weak acid is lowered in the electronically excited state.<sup>3</sup> However, the ESHT reaction has been computationally predicted and experimentally confirmed in many systems including phenol,<sup>4,7</sup> halogenated phenols,<sup>8,9</sup> methylphenol,<sup>10</sup> thiophenol,<sup>11-13</sup> pyrrole,<sup>14</sup> indole,<sup>15</sup> and 3-methyl-indole.<sup>16</sup>

The ESHT reaction of phenol is driven by a  $\pi\sigma^*$  state that is repulsive along the O-H bond. The  $\pi\sigma^*$  state results from the transition of an electron from the ring  $\pi$  orbital to the  $\sigma^*$  orbital localized in the hydroxyl group. However, as the overlap between the  $\pi$  orbital and the  $\sigma^*$  orbital is nearly zero, the  $\pi\sigma^*$  state is optically dark with zero oscillator strength. The molecule is initially excited to the  $\pi\pi^*$  state by absorption of a UV photon, then the  $\pi\sigma^*$  state is populated by crossing of the  $\pi\pi^*$  and the  $\pi\sigma^*$  states. In other words, predissociation of the  $\pi\pi^*$  state occurs by coupling to the  $\pi\sigma^*$  state. As O-H distance gets longer, there is a chance of second crossing with the ground ( $S_0$ ) state. When there is a crossing between the  $\pi\sigma^*$  and the  $S_0$  states, the system goes back to the ground state, i.e. internal conversion (IC) occurs. Without crossing, the system continues to evolve on the  $\pi\sigma^*$  surface and the hydrogen atom is detached. Thus the  $\pi\sigma^*$  state plays an important role as a bridge between the photoexcited state and the ground state. The first crossing ( $\pi\pi^*$ - $\pi\sigma^*$ ) determines the lifetime of the  $S_1$  state, and the second crossing ( $\pi\sigma^*$ - $S_0$ ) determines the fate of the dissociating hydrogen atom.

In the  $\pi\sigma^*$  state, the electron density is shifted from the  $\pi$  orbital of the aromatic ring to the diffuse  $\sigma^*$  orbital largely

localized on the leaving H atom, giving the  $\pi\sigma^*$  state of phenol a very high dipole moment of 10 Debye at the ground state optimized geometry.<sup>17</sup> As the O-H bond is ruptured, the  $\sigma^*$  orbital collapses to the 1s orbital of the hydrogen atom and the dipole moment decreases. Due to the high dipole moment the properties of the  $\pi\sigma^*$  state, e.g. the energy, its coupling to the optically active  $\pi\pi^*$  state, and the barrier to the crossing, are greatly affected by environment and substitution. For example, the external electric field effect on the  $\pi\sigma^*$  state of indole was computationally investigated, and it was found that the energy of the  $\pi\sigma^*$  state can be lower than the  $\pi\pi^*$  state depending on the strength and the direction of the electric field.<sup>18</sup> In this study, we computationally investigated the effects of amino group substitution on the ESHT reaction of phenol. By substituting an electron-donating group to phenol, the effect of internal electronic change on the  $\pi\sigma^*$  state and the ESHT reaction is investigated.

## Computational Method

Gaussian 03 package<sup>19</sup> was used for geometry optimization and calculation of the excited state energy. Ground state geometries of phenol and *ortho*-, *meta*-, and *para*-aminophenols were optimized at the MP2 level with 6-311++G basis set. The excited states of phenol and substituted phenols were calculated using the time-dependent density functional theory (TDDFT) with B3LYP functional and 6-311++G basis set. To get the potential energy (PE) profiles of the ground,  $\pi\pi^*$ , and  $\pi\sigma^*$  states along the O-H coordinate, O-H distance was increased by 0.1 Å step and the TDDFT calculation was repeated. The other coordinates were fixed at the ground-state optimized values during this repeated calculation. At each point on the O-H coordinate, molecular orbitals were visualized using Molekel<sup>20</sup> to identify which type of transition occurs for each electronic transition. When an electronic transition occurs from a delocalized orbital on the ring to a diffuse orbital localized on the hydroxyl group with a node between O and H, the

transition is labeled as a  $\pi\sigma^*$  transition.

### Results and Discussion

The excited states of phenol have been calculated to compare the accuracy of the current calculation with experimental data and higher-level computational results. Figure 1(a) shows the shape of the  $\sigma^*$  orbital at the ground state optimized geometry where the O-H distance is 0.977 Å. Due to the node between O and H, it shows a repulsive character when the  $\sigma^*$  orbital is populated in the  $\pi\sigma^*$  state. Figure 1(b) shows the PE profile of phenol along the O-H coordinate. The ground and excited state energies were calculated at the ground state optimized geometry ( $R_{OH} = 0.977$  Å) and the O-H distance ranging from 1.0 to 2.0 Å at 0.1 Å step. The vertical excitation energy of the  $S_1$  ( $\pi\pi^*$ ) state of phenol have been calculated to be 5.06 eV, which is 0.55 eV higher than the experimental value of  $36346.7\text{ cm}^{-1}$  (4.51 eV).<sup>17</sup> The vertical excitation energy of the lowest  $\pi\sigma^*$  state is 5.22 eV at this level of theory, 0.55 eV lower than the energy calculated by the CASPT2 method.<sup>17</sup> The results are summarized in Table 1. This level of

theory depicts the lowest  $\pi\pi^*$  and  $\pi\sigma^*$  states as nearly overlapped, though it is not compatible with previous experimental and computational studies. It is known that the TDDFT method has a drawback in the calculation of charge transfer states.<sup>21</sup> As the  $\pi\sigma^*$  state has a charge transfer character near the ground state geometry, it is expected that this calculation should have relatively large error in the energy of the  $\pi\sigma^*$  state. Nevertheless this study gives relative and qualitative results for the purpose of comparison between phenol and substituted phenols in the ESHT reaction. Similar amount of relative errors should

**Table 1.** TDDFT vertical excitation energies of the lowest  $\pi\pi^*$  and  $\pi\sigma^*$  states of phenol and aminophenols.

|                       | vertical excitation energy (eV) |               |
|-----------------------|---------------------------------|---------------|
|                       | $\pi\pi^*$                      | $\pi\sigma^*$ |
| phenol                | 5.06                            | 5.22          |
| <i>o</i> -aminophenol | 4.72                            | 5.14          |
| <i>m</i> -aminophenol | 4.34                            | 4.65          |
| <i>p</i> -aminophenol | 4.28                            | 4.44          |

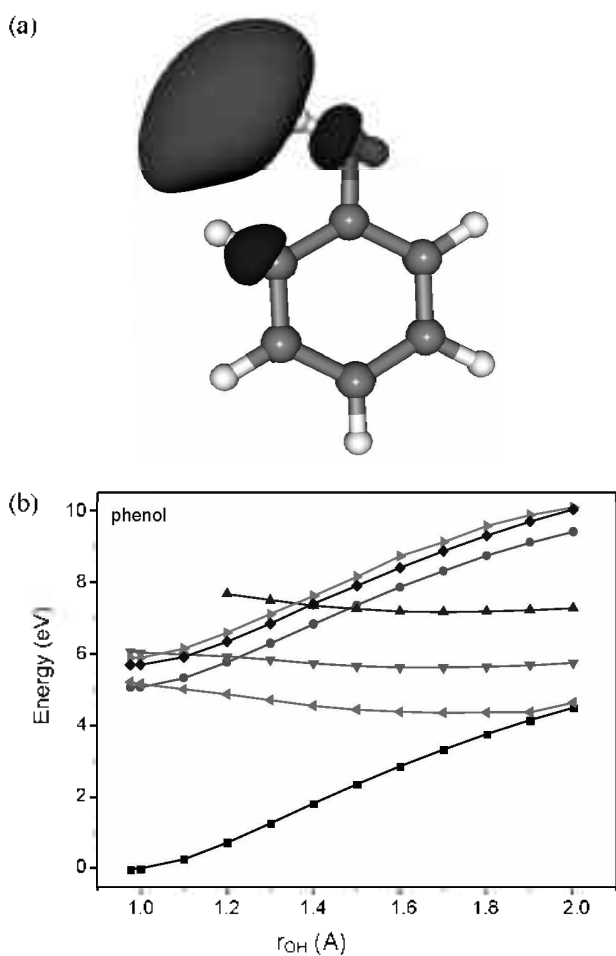


**Figure 1.** (a) Optimized geometry of phenol and the  $\sigma^*$  orbital. (b) TDDFT potential energy profile of phenol: ■, ground state; ●, first  $\pi\pi^*$  excited state; ◆, second  $\pi\pi^*$  excited state; ▶, third  $\pi\pi^*$  excited state; ◀, first  $\pi\sigma^*$  excited state; ▼, second  $\pi\sigma^*$  excited state; ▲, third  $\pi\sigma^*$  excited state.

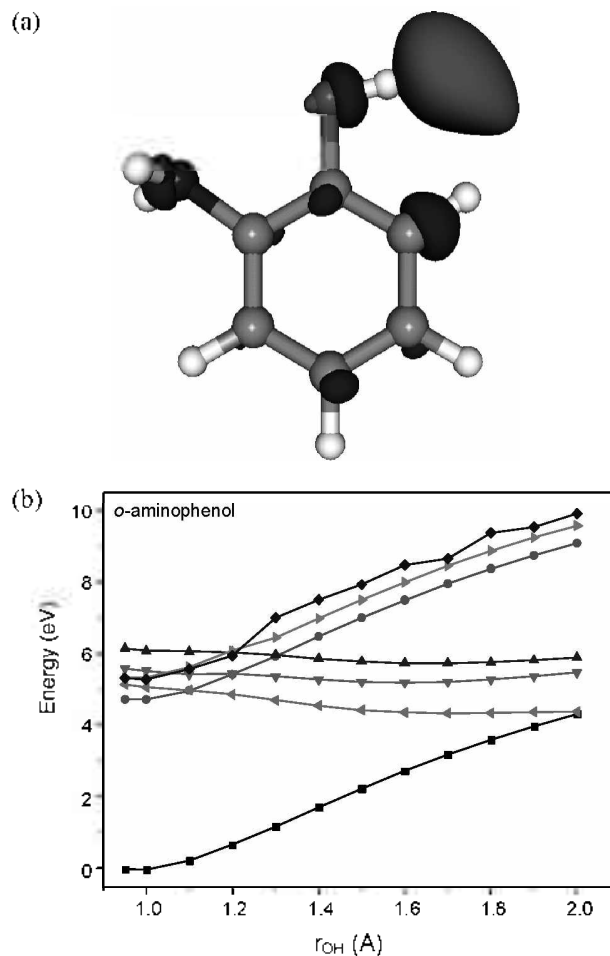


**Figure 2.** (a) Optimized geometry of *o*-aminophenol and the  $\sigma^*$  orbital. (b) TDDFT potential energy profile of *o*-aminophenol. Excited states are labeled in the same way as in Figure 1(b).

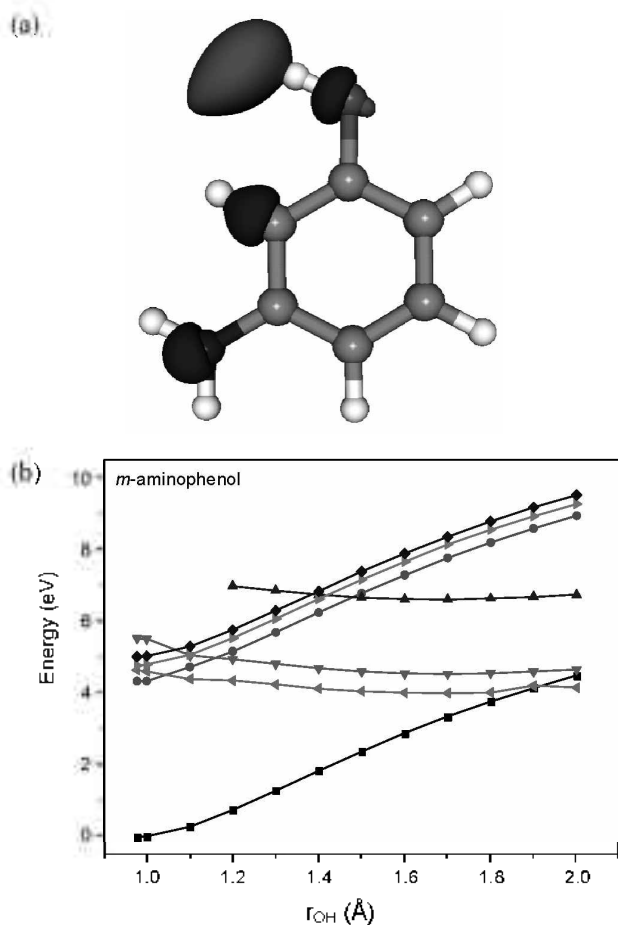


**Figure 3.** (a) Optimized geometry of *m*-aminophenol and the  $\sigma^*$  orbital. (b) TDDFT potential energy profile of *m*-aminophenol. Excited states are labeled in the same way as in Figure 1(b).

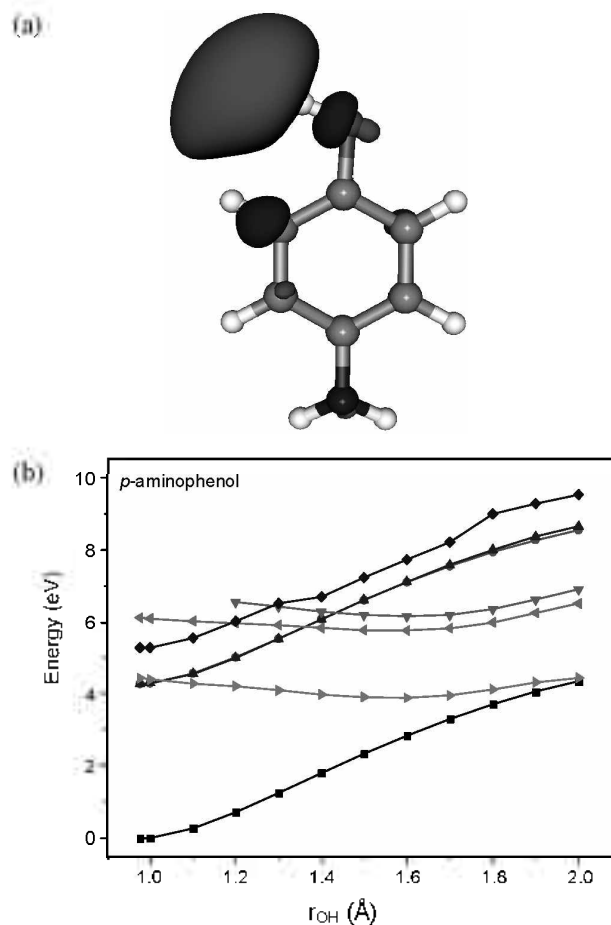


**Figure 4.** (a) Optimized geometry of *p*-aminophenol and the  $\sigma^*$  orbital. (b) TDDFT potential energy profile of *p*-aminophenol. Excited states are labeled in the same way as in Figure 1(b).

be assumed in the subsequent calculation of substituted phenol compounds.

Lines were drawn between points that belong to the same electronic states, by checking the shapes of the orbitals. The PE profile in Figure 1(b) qualitatively reproduces the previous CASSCF/CASPT2 calculation in the sense that it shows a bound  $\pi\pi^*$  state and a repulsive  $\pi\sigma^*$  state.<sup>17</sup> Three lowest transitions of each type are shown to compare the result of phenol with other substituted phenols.

It would have been better to use a method that could optimize the geometry of the excited state, e.g. CASSCF or CASPT2, and to obtain the exact minimum energy path of the ESHT reaction. However the less computationally demanding TDDFT calculation at the ground-state optimized geometry gave acceptable qualitative results for the excited states of adenine.<sup>22</sup> Furthermore, as we are concerned with the dissociation of a light H atom, other nuclear motions are supposed to be much slower than the motion along the O-H coordinate. It is not a poor approximation that the other coordinates are frozen during the dissociation along the O-H coordinate.

Figure 2 shows the computational results of *o*-aminophenol. Two stable isomers exist depending on the orientation of the OH group with respect to the amino group: *cis*- and *trans*-isomers. In the *cis*-isomer there is an internal hydrogen bonding

between the hydroxyl hydrogen and the amino nitrogen. Though the *cis*-isomer is more stable due to the strong internal hydrogen bonding, this isomer does not contribute to the ESHT reaction because the hydroxyl hydrogen is tightly bound to the amino group. Only the *trans*-isomer was considered in this study for the purpose of comparing ESHT reactions. Figure 2(a) is the shape of the  $\sigma^*$  orbital at the ground state optimized geometry of *o*-aminophenol in the *trans* form. The OH group faces away from the amino group at the *ortho* position. As in Figure 1(a) the nodal plane between O and H indicates the repulsive nature of the  $\pi\sigma^*$  state. Figure 2(b) is the PE profile of *o*-aminophenol along O-H coordinate. The vertical excitation energies of phenol and *o*-aminophenol show small difference. The lowest  $\pi\pi^*$  state in *o*-aminophenol is 0.3 eV lower than that of phenol and the lowest  $\pi\sigma^*$  state is only 0.1 eV lower. However, when Figure 2(b) is compared to Figure 1(b), it is readily seen that the lowest three  $\pi\sigma^*$  states are closer in energy in *o*-aminophenol than in phenol.

Figures 3 and 4 show the results of *m*- and *p*-aminophenols, respectively. For *m*-aminophenol, there are also *cis*- and *trans*-isomers. The result of the more stable *cis*-aminophenol is shown here, but *trans*-aminophenol also shows similar behavior. For non-planar *m*- and *p*-aminophenols, there is a strong mixing between excited states near the crossing points

and it was difficult to classify a certain transition as  $\pi\pi^*$  or  $\pi\sigma^*$  type. In such a case, the mixed transition was labeled with the one with the larger orbital coefficient. Again Figures 3(a) and 4(a) confirm the antibonding nature of the  $\pi\sigma^*$  state in each phenol derivative. Figure 3(b) shows that the lower two  $\pi\sigma^*$  states are close and the third  $\pi\sigma^*$  state lies a bit higher in *m*-aminophenol, while one  $\pi\sigma^*$  state lies in low and two higher  $\pi\sigma^*$  states are close in Figure 4(b) of *p*-aminophenol. The first and second  $\pi\pi^*$  states of *p*-aminophenol are very close and the two curves nearly overlap with each other, making it difficult to distinguish the two. Table 1 shows that vertical excitation energies of  $\pi\pi^*$  and  $\pi\sigma^*$  states are very close in each phenol derivative at this level of theory. Also it indicates that as amino group is introduced to phenol, excited states are lowered in general. The substitution at the *para* position has the largest lowering effect that becomes smaller as the amino group is moved closer to the hydroxyl group. On the other hand, the energy gap between the lowest  $\pi\pi^*$  and  $\pi\sigma^*$  states increases as the amino group comes close to the hydroxyl group.

Comparison of PE profiles of phenol and substituted phenols gives a qualitative picture of the effect of amino substitution on the ESHT reaction of phenol. As the electron donating amino group (-NH<sub>2</sub>) comes close to the hydroxyl group (-OH), more  $\pi\sigma^*$  states overlap with  $\pi\pi^*$  states. It is seen that *o*-aminophenol has three low-lying  $\pi\sigma^*$  states and seems to have an efficient ESHT reaction through many dissociation channels along the repulsive  $\pi\sigma^*$  states. On the other hand, *p*-aminophenol has the lowest  $\pi\sigma^*$  state and the smallest gap between  $\pi\pi^*$  and  $\pi\sigma^*$  states. This might give *p*-aminophenol a higher chance of undergoing the ESHT reaction. Therefore the amino substitution enhances the ESHT reaction of phenol in all substitution positions according to the current computational study, and more efficient fluorescence quenching is expected in amino substituted phenols. It is interesting to note that Fujii's group has carried out the electronic spectroscopic study of fluorophenol-ammonia clusters to estimate that the ESHT reaction becomes faster in the order of *m*-, *p*-, and *o*-fluorophenol.<sup>8</sup> Substitution by halogen has an electron-withdrawing effect, while an amino group is a typical electron-donating one. It will be interesting to investigate the effect of an electron withdrawing group, such as a nitro group, in the ESHT reaction using an electronic structure calculation method.

### Conclusion

The excited states of amino substituted phenols were studied by TDDFT calculation. All three amino-substituted phenols have dissociative  $\pi\sigma^*$  states along the OH bonds as in phenol. The *o*-aminophenol has a slightly higher barrier to ESHT than phenol, but has more low-lying dissociative states that should help efficient quenching of the excited state. The *p*-aminophenol has the lowest gap between the  $\pi\pi^*$  state and the  $\pi\sigma^*$  state, while *m*-aminophenol lies between *o*- and *p*-derivatives. In general it was found that the amino substitution has an effect of enhancing the ESHT reaction and efficiently quenching the fluorescence of phenol.

Experimental verification of the substitution effect is currently underway. Electronic spectroscopy of *p*-aminophenol<sup>23-27</sup> and *m*-aminophenol<sup>28,29</sup> has already been investigated. Based on the previous studies, the product of the ESHT reaction between the amino substituted phenols and ammonia in the gas phase will be observed using two-color REMPI spectroscopy. After exciting the cluster of substituted phenol and ammonia (H<sub>2</sub>N-Ph-OH-(NH<sub>3</sub>)<sub>n</sub>) to its S<sub>1</sub> state by a first laser, the metastable hydrogen-transferred product (ammonium radical solvated by ammonia, NH<sub>4</sub>(NH<sub>3</sub>)<sub>n-1</sub>) will be detected using a second laser. This study will provide a better understanding of the fluorescence property of proteins and possibly a better way to utilize it.

**Acknowledgments.** This work was supported by the Korea Research Foundation Grant funded by the Korean Government (MOEHRD, Basic Research Promotion Fund) (KRF-2008-331-C00132) and the Ajou University Research Grant (20083970).

### References

- Sobolewski, A. L.; Domcke, W.; Dedonder-Lardeux, C.; Juvet, C. *Phys. Chem. Chem. Phys.* **2002**, *4*(7), 1093.
- David, O.; Dedonder-Lardeux, C.; Juvet, C. *Intl. Rev. Phys. Chem.* **2002**, *21*(3), 499.
- Svage, J. A. *J. Phys. Chem.* **1995**, *99*(16), 5772.
- Pino, G. A. *et al. J. Chem. Phys.* **1999**, *111*(24), 10747.
- Grégoire, G. *et al. J. Phys. Chem. A* **2000**, *104*, 9087.
- Pino, G. *et al. Phys. Chem. Chem. Phys.* **2000**, *2*(4), 893.
- Grégoire, G. *et al. J. Phys. Chem. A* **2001**, *105*, 5971.
- Tsuji, N. *et al. Phys. Chem. Chem. Phys.* **2006**, *8*(1), 114.
- Devine, A. L.; Nix, M. G. D.; Cronin, B.; Ashfold, M. N. R. *Phys. Chem. Chem. Phys.* **2007**, *9*(28), 3749.
- King, G. A. *et al. Phys. Chem. Chem. Phys.* **2008**, *10*(42), 6417.
- Lim, I. S.; Lim, J. S.; Lee, Y. S.; Kim, S. K. *J. Chem. Phys.* **2007**, *126*(3).
- Lim, J. S. *et al. Angew. Chem. Int. Ed.* **2006**, *45*(38), 6290.
- Devine, A. L.; Nix, M. G. D.; Dixon, R. N.; Ashfold, M. N. R. *J. Phys. Chem. A* **2008**, *112*(39), 9563.
- David, O. *et al. J. Chem. Phys.* **2004**, *120*(21), 10101.
- Dedonder-Lardeux, C.; Grosswasser, D.; Juvet, C.; Martenichard, S. *Phys. Chem. Comm.* **2001**, *4*, 21.
- David, O.; Dedonder-Lardeux, C.; Juvet, C.; Sobolewski, A. L. *J. Phys. Chem. A* **2006**, *110*(30), 9383.
- Sobolewski, A. L.; Domcke, W. *J. Phys. Chem. A* **2001**, *105*(40), 9275.
- Dedonder-Lardeux, C.; Juvet, C.; Pertun, S.; Sobolewski, A. L. *Phys. Chem. Chem. Phys.* **2003**, *5*(22), 5118.
- Frisch, M. J. *et al. Gaussian 03*; Gaussian, Inc.: Wallingford CT, 2004.
- Flükiger, H. P.; Lüthi, S.; Portmann, J. W. *MOLEKEL*, *5*:3; Swiss National Supercomputing Centre CSCS: Manno (Switzerland), 2000.
- Dreuw, A.; Head-Gordon, M. *J. Am. Chem. Soc.* **2004**, *126*(12), 4007.
- Sobolewski, A. L.; Domcke, W. *Eur. Phys. J. D* **2002**, *20*(3), 369.
- Mori, H. *et al. Chem. Phys.* **2002**, *277*(2), 105.
- Gerhards, M.; Unterberg, C. *Appl. Phys. A* **2001**, *72*, 273.
- Jansen, A.; Gerhards, M. *J. Chem. Phys.* **2001**, *115*(12), 5445.
- Meenakshi, P. S.; Biswas, N.; Wategaonkar, S. *J. Chem. Phys.* **2002**, *117*(24), 11146.
- Wategaonkar, S.; Doraiswamy, S. *J. Chem. Phys.* **1996**, *105*(5), 1786.
- Robinson, T. W. *et al. J. Phys. Chem. A* **2004**, *108*(20), 4420.
- Shinozaki, M. *et al. Phys. Chem. Chem. Phys.* **2003**, *5*(22), 5044.